

# Detection and Abundance Estimation of Material Classes from Airborne LWIR Hyperspectral Data

L. J. Richards <sup>(1)</sup>, A. Gammerman <sup>(2)</sup>, and I. Nouretdinov <sup>(2)</sup>

<sup>(1)</sup> QinetiQ, Room 2022, A5 Building, Cody Technology Park, Ively Road, Farnborough, Hampshire GU14 0LX, UK [ljrichards@QinetiQ.com](mailto:ljrichards@QinetiQ.com)

<sup>(2)</sup> Universal Prediction, 9 Greenacre Court, Egham, Surrey TW20 0RF, UK [alex@universal-prediction.com](mailto:alex@universal-prediction.com)

## Abstract

*The paper investigates usage of kernel ridge regression techniques to estimate the abundances of pre-specified material classes in LWIR hyperspectral data. Experiments are presented using library training spectra and selected test data from an airborne trial at Kirkcudbright. The technique can be extended to provide a material detector for each class. A leave-one-out ROC analysis has been used to quantify the discrimination of the training data. The techniques of conformal prediction can be used to derive a valid confidence interval for each abundance estimate, requiring only minimal statistical assumptions.*

## Introduction

Previous work [1] has suggested that it is possible to estimate the abundances of pre-defined material classes from hyperspectral measurements in the visible and Near IR spectral bands. This can be done by using ridge regression techniques. A further study has therefore been performed, to investigate whether these techniques can be extended for use in the LWIR band – a band that is attractive in offering a day/night facility.

### Ridge regression [2]

Suppose that we have a set of training feature vectors  $x_1, x_2, \dots, x_T$ , each vector containing a set of hyperspectral measurements. Suppose too that each training vector relates to a pure pixel, i.e. the pixel is known to belong to one and only one material class. Consider any one class. Let  $y$  be a vector whose  $t$ 'th element is the abundance (i.e. proportion) for the given class of the  $t$ 'th training vector ( $t = 1, \dots, T$ ). Then  $y$  is known, because if the  $t$ 'th training vector belongs to the given class, we have  $y_t = 1$ ; otherwise  $y_t = 0$ . Now suppose we are given a test feature vector,

$x$ , for a pixel that may contain more than one type of material. We wish to calculate  $\hat{y}$ , the estimated value of the abundance (for the specified class) of the test pixel. The required formula is:

$$\hat{y} = y'(K + aI)^{-1}k \quad (1)$$

where the dash denotes transpose,  $I$  denotes the  $T \times T$  unit matrix,  $a$  is a small positive scalar, known as the ridge factor,  $K$  is a  $T \times T$  matrix such that

$$K_{st} = \kappa(x_s, x_t) \quad (s, t = 1, \dots, T)$$

$k$  is a vector such that

$$k_t = \kappa(x_t, x) \quad (t = 1, \dots, T)$$

and  $\kappa$  is a suitable kernel function. In the simplest case, the kernel just evaluates the dot product of the two vectors, i.e.

$$\kappa(u, v) = u \cdot v.$$

Other choices of kernel function are possible. It has been found by experiment that a suitable choice is a low order polynomial, i.e.

$$\kappa(u, v) = (u \cdot v + 1)^d$$

with the order,  $d$ , being less than or equal to 5, say. Equation (1) is applied separately for every choice of class, thus building up a vector of abundance estimates, one per class. Any estimate below zero is set to zero; any estimate above 1 is set to 1. The revised abundances are then divided by their sum, to ensure that they sum to 1.

### Training and test spectra

Training spectra were taken from the ‘ASTER’ public domain spectral library [3]. The classes used were: ‘soil’, ‘manmade’, ‘solid rock’, ‘powder rock’ and ‘vegetation’. Test spectra were taken from hyperspectral emissivity measurements made using the AHI airborne sensor in a trial at Kirkcudbright Ranges, in June 2004. The 160 measurement bands available were reduced to 23, between 8.5 and 11.2 microns. To compare the reflectance of the training data with the emissivity of the test data, it was assumed that emissivity = 1 – reflectance. The emissivity values used were produced from the raw measurements using an atmospheric correction process.

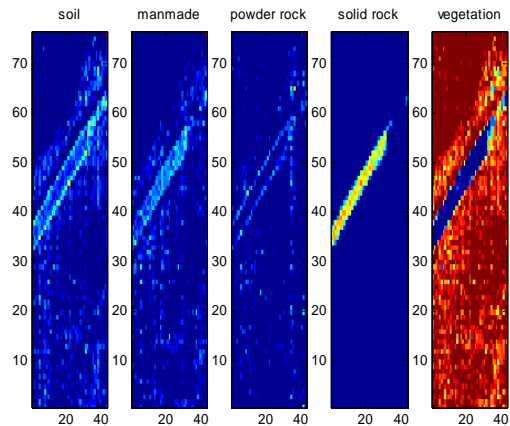
### Test results for abundances

Figure 1 shows an atmospherically-corrected emissivity image relating to one wavelength (9.2233 microns). The diagonal structure is a track. The area above and to the left of the track was a field, with hay stacked on top of the grass. Below and to the right of the track was a woodland region.



**Figure 1: Emissivity image at 9.2233  $\mu\text{m}$**

Four data sets of AHI measurements were used and abundance estimates calculated using ridge regression. Figure 2 shows the results for one data set in which the track can be seen, and is judged to contain mostly solid rock; the other two areas are judged to contain mostly vegetation.



**Figure 2: Abundance estimates for data set Z5, 3rd order polynomial kernel, 157 spectra per class. (Blue = 0; brown = 1)**

### Material detection

In some circumstances, the main concern may be not so much to produce precise abundance estimates, but rather to decide what types of materials are present. One would wish to make a yes-or-no decision, for each class, as to whether any material of that class is present in a given pixel. This could be achieved by comparing the abundance estimate for a given class against a threshold (maybe class-dependent); the material is declared to be present if and only if the estimate exceeds the threshold.

In order to investigate this possibility, a leave-one-out analysis was performed, using training data only. The estimation algorithm was run 20 times. In each case, one of the 20 training vectors (four randomly chosen from each of 5 classes), was omitted, and the omitted vector used as a test vector. In each case, it was noted, for each class, and for each of a set of threshold values, whether there was a correct detection for that class, and whether there was a false alarm for that class. This

procedure was repeated 1000 times, with different random choices of which library spectra were to be included in the training spectra. By counting the numbers of correct detections and false alarms, and dividing by the number of opportunities for correct detections and false alarms, the probability of detection (PD) and the probability of false alarm (PFA) could be calculated. Figure 3 shows an example for one class ('soil') of the dependency of PD and PFA on threshold. Plotting PD versus PFA gave the ROC curve shown in figure 4.

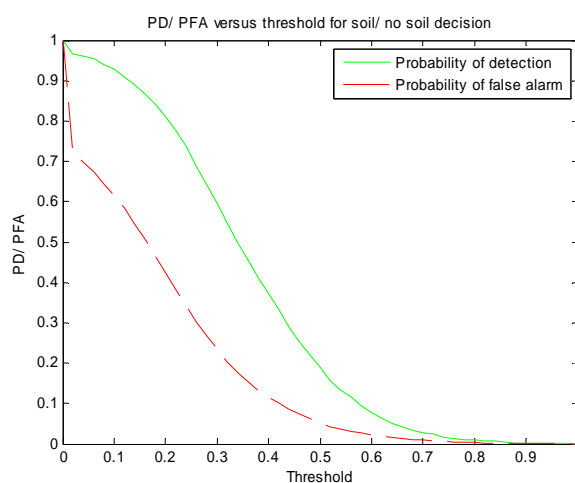


**Figure 3: Variation of PD and PFA with threshold, for class 'soil'**

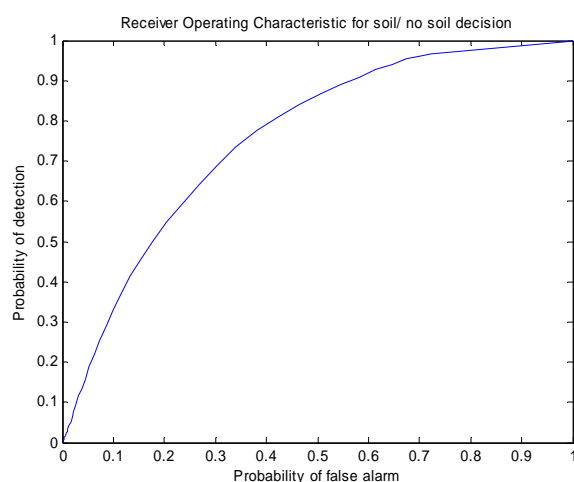


**Figure 4: Receiver Operator Characteristic for 'soil' class**

The curve for 'soil' is reasonable: some other classes have worse performance. The performance of each curve can be quantified using the Area Under the Curve (AUC). Table 1 shows the AUC for each class.

Class	AUC
1: Soil	0.76
2: Manmade	0.49
3: Powder rock	0.51
4: Solid rock	0.86
5: Vegetation	0.77
Average	0.68

**Table 1: AUC by class (5 classes)**

From these figures, solid rock appears the best class, and manmade the worst. Another analysis method is pair-wise discriminability, where one considers just two classes at a time, and takes the average AUC of the two ROC curves produced. Table 2 shows that the hardest pair of classes to discriminate between is manmade and powder rock.

Class	2	3	4	5
1	0.69	0.66	0.94	0.78
2		0.49	0.80	0.78
3			0.84	0.62
4				0.94

**Table 2: Pair-wise AUCs**

### Conformal prediction: the ridge regression confidence machine

The techniques of conformal prediction [4], [5], [6], [7] can be used to provide a confidence interval for each abundance estimate, for each class. The ‘confidence machine’ – the algorithm that calculates the prediction and provides confidence intervals – has a number of advantages:

- It gives valid results, i.e. it never overrates the accuracy and reliability of its predictions.
- It has a wide variety of applications, since it requires only one assumption – that the examples analysed are independent and identically distributed, according to the same probability distribution (we do not need to know what that distribution is).
- The algorithm can be applied to both low-dimensional and high-dimensional data.

One of the advantages of the method is that the user can control accuracy of prediction by selecting the required confidence level.

#### Confidence machine results

According to table 1, classes ‘manmade’ and ‘powder rock’ are the most difficult to distinguish from others. We now investigate what would happen if we were to delete these classes, and make the simplifying assumption that in a particular scenario they are absent. (This is just to illustrate the potential improvement in performance: the assumption may not be justified in a realistic scenario. Figure 2 suggests that the amounts of manmade and powder rock materials present in the Kirkcudbright data are relatively small.) We are left with three classes, which now have the AUC values shown in table 3.

Class	AUC
Soil	0.88
Solid rock	0.92
Vegetation	0.88
Average	0.89

**Table 3: AUC, by class (3 classes)**

We attempt to detect these classes using a 3<sup>rd</sup> order polynomial kernel, with 58 spectra per class. We apply the confidence machine with a confidence level of 90%. Figure 5 shows the estimated abundances. Figures 6 and 7 show the lower and upper 90% confidence bounds. (That is, in a large number of experiments, the true abundance would be greater than or equal to the lower bound and less than or equal to the upper bound on at least 90% of occasions.) The 90% level was chosen arbitrarily – other levels such as 95% or 99% could be used if desired. The higher the level, the wider the interval will be.

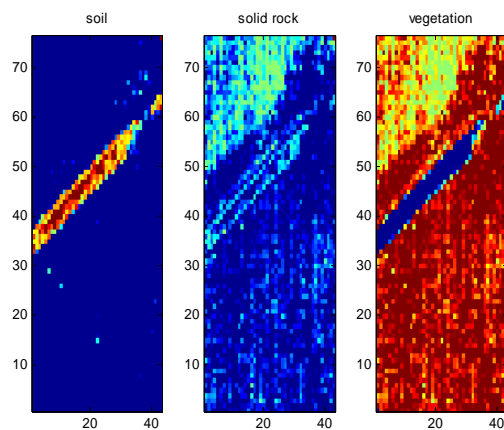


**Figure 5: Estimated abundances, 3 classes, 58 spectra per class, 3<sup>rd</sup> order polynomial kernel, data set Z5**

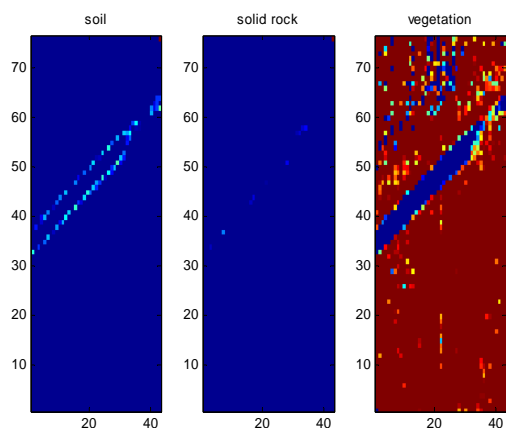


**Figure 6: Lower bounds on abundances for 90% confidence interval**

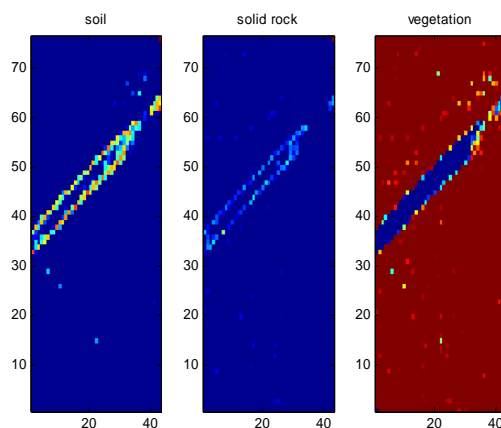


**Figure 8: Lower bounds on abundances for 50% confidence interval**

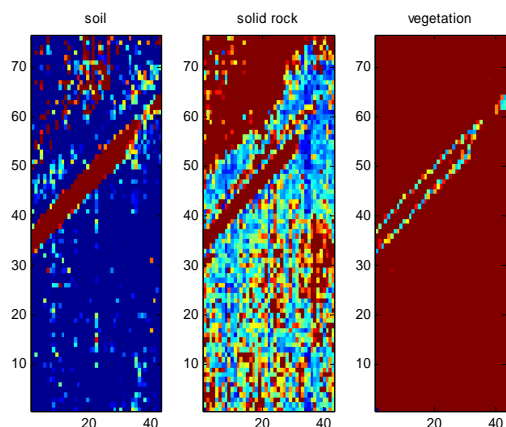


**Figure 7: Upper bounds on abundances for 90% confidence interval**

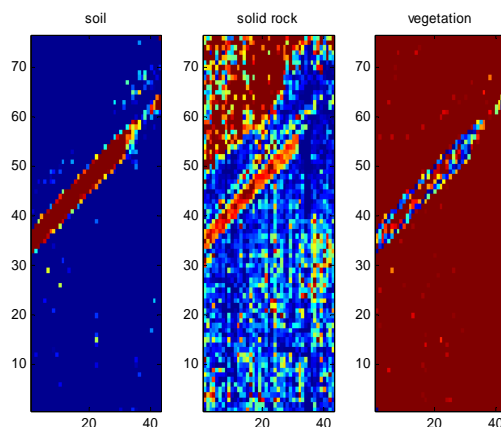


**Figure 9: Upper bounds on abundances for 50% confidence interval**

The pixels inside the track generally have a lower bound of 0 and an upper bound of 1, for all classes, so the estimator is unsure of the abundances, at this confidence level.

For vegetation, in the area below the track, we generally have lower bound = upper bound = 1, so the estimator has high confidence that this area contains vegetation.

If the confidence level is now reduced from 90% to 50% the lower and upper bounds are given by figures 8 and 9, respectively.

The lower and upper bounds are now closer together, but the effect on the classification is small. The confidence machine is still very uncertain as to the composition of the track, though from figure 5 its clear best estimate is that it consists mainly of soil. As before, we are confident that the area below the track is vegetation. The most pronounced change is that we are now 'sure' (at the 50% level) that the area above the track is vegetation throughout. The track area in figure 9 has scattered blue pixels, so there is now a suggestion that

whatever the track is mainly composed of, it doesn't contain much vegetation.

It has been seen that the confidence interval is not always as narrow as might be desired, so that it is not always possible to give a confident decision as to the types of materials present in a given area. However, this is not necessarily the fault of the algorithms. It may be that a better set of classes would give better performance. It may also be that the training spectra are not representative of the test spectra.

### Summary

(a) The kernel ridge regression algorithm appears to be a convenient and robust method of estimating abundances. The choice of adjustable parameters (kernel type and ridge factor) is not critical.

(b) The abundance estimates can be compared with a threshold to provide a material detection algorithm, for each class. The effectiveness of the detector can be assessed from the training data using a leave-one-out ROC analysis. This can suggest those classes that should be discarded, if possible.

(c) The ridge regression confidence machine is a powerful algorithm that can provide valid confidence intervals at any user-specified confidence level, for each abundance estimate, based on only minimal statistical assumptions.

(d) Performance of the estimation algorithm is constrained by the discriminability of the training data and the similarity or otherwise of the test data to the training data. Further work could usefully be done to investigate methods of defining a good set of classes.

### Acknowledgements

The work reported in this paper was funded by the Electro-magnetic Remote Sensing (EMRS) Defence Technology Centre, established by the UK Ministry of Defence

and run by a consortium of SELEX Galileo, Thales UK and Roke Manor Research.

### References

1. A. Pratt and J. Nothard, "Nonlinear unmixing of hyperspectral imagery using kernel techniques", 5<sup>th</sup> EMRS DTC technical conference – Edinburgh 2008.
2. C. Saunders, A. Gammerman and V. Vovk, "Ridge regression learning algorithm in dual variables", in *Proceedings of the 15<sup>th</sup> International Conference on Machine Learning, ICML'98*.
3. A.M. Baldridge, S.J. Hook, C.I. Grove and G. Rivera, The ASTER Spectral Library Version 2.0, [http://speclib.jpl.nasa.gov/downloads/SE\\_D\\_08\\_00553.pdf](http://speclib.jpl.nasa.gov/downloads/SE_D_08_00553.pdf). NOTE: Version 1.0 was used.
4. A. Gammerman and V. Vovk, "Prediction algorithms and confidence measures based on algorithmic randomness theory", *Theoretical Computer Science*, 287, pp. 209-217 (2002)
5. I. Nourtdinov, T. Melluish and V. Vovk, "Ridge regression confidence machine", in *Proceedings of the ICML'2001*.
6. A. Gammerman and V. Vovk, "Hedging Predictions in machine learning", *Computer Journal*, Vol. 50, No 2, pp.151-163(2007); doi: 10.1093/comjnl/bx1065/  
<http://comjnl.oxfordjournals.org/cgi/content/abstract/50/2/151>
7. V. Vovk, A. Gammerman and G. Shafer, "Algorithmic learning in a random world", Springer, 2005.